British Journal of Pharmacology

British Journal of Pharmacology (2019) **176** 317–333 317

RESEARCH PAPER

Seselin ameliorates inflammation *via* targeting Jak2 to suppress the proinflammatory phenotype of macrophages

Correspondence Qiang Xu and Xudong Wu, State Key Laboratory of Pharmaceutical Biotechnology, School of Life Sciences, Nanjing University, 163 Xianlin Avenue, Nanjing 210023, China. E-mail: molpharm@163.com; xudongwu@nju.edu.cn

Received 27 March 2018; **Revised** 23 August 2018; **Accepted** 24 September 2018

Lili Feng[1,*], Yi Sun[1,*], Pingping Song[2,*], Lisha Xu[1], Xingxin Wu[1], Xuefeng Wu[1], Yan Shen[1], Yang Sun[1], Lingdong Kong[1], Xudong Wu[1] and Qiang Xu[1]

[1]*State Key Laboratory of Pharmaceutical Biotechnology, Department of Rheumatology and Immunology, Nanjing Drum Tower Hospital, School of Life Sciences, Nanjing University, Nanjing, China, and* [2]*Jiangsu Centre for Research and Development of Medicinal Plants, Institute of Botany Jiangsu Province, Chinese Academy of Sciences, Nanjing, China*

*These authors contributed equally to this work.

BACKGROUND AND PURPOSE

Sepsis is a serious clinical condition with a high mortality rate. Anti inflammatory agents have been found to be beneficial for the treatment of sepsis. Here, we have evaluated the anti-inflammatory activity of seselin in models of sepsis and investigated the underlying molecular mechanism(s).

EXPERIMENTAL APPROACH

In vivo therapeutic effects of seselin was evaluated in two models of sepsis, caecal ligation and puncture or injection of LPS, in C57BL/6 mice. *In vitro,* anti-inflammatory activity of seselin was assessed with macrophages stimulated with LPS and IFN-γ. Anti inflammatory actions were analysed with immunohistochemical methods, ELISA and Western blotting. Flow cytometry was used to assess markers of macrophage phenotype (pro- or anti-inflammatory). Other methods used included co-immunoprecipitation, cellular thermal shift assay and molecular docking.

KEY RESULTS

In vivo, seselin clearly ameliorated sepsis induced by caecal ligation and puncture. In lung tissue from septic mice and in cultured macrophages, seselin down-regulated levels of proinflammatory factors and activity of STAT1 and p65, the master signal pathway molecules for polarization of macrophages into the proinflammatory phenotype. Importantly, adoptive transfer of bone marrow-derived macrophages, pretreated with seselin, lowered systemic proinflammatory factors in mice challenged with LPS. The underlying mechanism was that seselin targeted Jak2 to block interaction with IFNγ receptors and downstream STAT1.

CONCLUSIONS AND IMPLICATIONS

Seselin exhibited anti-inflammatory activity through its action on Jak2. These results indicated a possible application of seselin to the treatment of inflammatory disease *via* blocking the development of the proinflammatory phenotype of macrophages.

Abbreviations

BALF, bronchoalveolar lavage fluid; BMDMs, bone marrow-derived macrophages; CETSA, cellular thermal shift assay; CFSE, carboxyfluorescein diacetate succinimidyl ester; CLP, caecal ligation and puncture; co-IP, co-immunoprecipitation; IHC, immunohistochemistry; IKK, IκB kinase; iNOS, inducible NO synthase; M-CSF, macrophage-colony stimulating factor; MPN, myeloproliferative neoplasm; MTT, 3-(4,5-dimethyl-2-thiazyl)-2,5-diphenyl-2*H*-tetrazoli-um bromide; PMA, phorbol 12-myristate 13-acetate; STAT1, signal transducer and activator of transcription 1; TLR4, toll-like receptor 4

DOI:10.1111/bph.14521

Introduction

Sepsis is a severe systemic inflammatory response with a high mortality (Martin *et al.*, 2003). Clinically diagnosed sepsis is characterized by the systemic inflammatory response syndrome induced by bacterial pathogen infection (Stearns-Kurosawa *et al.*, 2011). During the first few days in infected patients, macrophages are activated to phagocytize pathogens and to produce a range of proinflammatory factors (Benoit *et al.*, 2008). Unfortunately, the continued and unlimited activation of macrophages/monocytes and neutrophils further exacerbates the progression of the septic response (Stearns-Kurosawa *et al.*, 2011). The large amount and number of cytokines produced by these activated immune cells is always associated with severe organ dysfunction and higher mortality (Bozza *et al.*, 2007). Given that, restraint of the functional phenotype of macrophages and a rebalancing of the cytokine profile will be beneficial for the treatment of the corresponding inflammatory condition.

As the major mediators of inflammatory responses, macrophages are considered to polarize to the classically activated phenotype with proinflammatory features to garden host responses and to clear foreign organisms and cellular debris (Meylan *et al.*, 2006; Kotas and Medzhitov, 2015). These activated macrophages must be rapidly mobilized and equally rapidly de-activated to avoid tissue damage. Alternatively, macrophages can also be activated to produce anti-inflammatory factors and restore tissue integrity. However, enhancement of anti-inflammatory macrophages can lead to a poor prognosis in sepsis (Spellberg and Edwards, 2002; Rodgaard-Hansen *et al.*, 2014). Thus, a proper control of macrophage activation to maintain appropriate functional phenotype is crucial to protect against the progression of inflammatory diseases.

The polarization of macrophages is coordinated by a large range of mediators that form complex regulatory networks (Sica and Mantovani, 2012; Alvarez-Errico *et al.*, 2015; Jha *et al.*, 2015). Stimulated by different inducers, macrophages activate a range of signal pathways to elicit gene expression changes and gain the corresponding functional properties. Tissue-resident macrophages, shaped by metabolic stimuli, help to coordinate development and maintain microenvironment in a steady state (Glass and Natoli, 2016). Other danger signals are likely to modulate the functional polarization of macrophages *via* activating specific transcription factors. Microbial components, such as **LPS**, engage with **toll-like receptor 4 (TLR4)** to skew macrophages to the proinflammatory phenotype *via* the NF-κB signal pathway (Lawrence and Natoli, 2011). Similarly, exposure to **IFN-γ** triggered or aggravated the proinflammatory properties through the **Jak2-STAT1** pathway (Lawrence and Natoli, 2011). In contrast to IFN-γ, stimulation by **IL-4** triggered a different activation program involving STAT6 (Piccolo *et al.*, 2017). Because of the diverse phenotype and complex effects of macrophages, targeting key biological mediators and interfering with the functional properties have become promising therapeutic options for patients with inflammatory diseases. Based on these considerations, a range of inhibitors targeting various signal proteins have been developed and widely used as tools, such as **TAK-242 (resatorvid;** inhibitor of TLR4) (Matsunaga *et al.*, 2011) and ST-2825 (inhibitor of MyD88) (Hernanz *et al.*, 2015). Some others, like **ruxolitinib** or **tofacitinib** (inhibitors of Jaks), have been evaluated in clinical trials (Fleischmann *et al.*, 2012; Cervantes *et al.*, 2013). However, due to the potential side effects and/or high cost of these compounds, it is still necessary to search for more efficient drugs which have better safety and are easier to prepare.

In the present study, we have identified the anti-inflammatory activity of seselin, an angle-pyrancoumarin widely distributed in the plant kingdom. Seselin has been reported to have good antifungal activity (Cardenas-Ortega *et al.*, 2007) and derivatives with anti-bacterial activity (Melliou *et al.*, 2005). In plants, seselin has inhibitory activity on both indole acetic acid oxidase and peroxidase enzyme systems (Goren and Tomer, 1971). Seselin is effective against blowfly larvae (and its effects on the feeding and development of *Lucilia cuprina* larvae) and selectively activates some yeast strains (Siriwardhana *et al.*, 2015). It also has anti-inflammatory (Garcia-Argaez *et al.*, 2000), and antinociceptive (Lima *et al.*, 2006) properties. Although there are studies on its biological activity, the effects of seselin on sepsis and the underlying mechanism(s) are still unknown. Our findings suggested that seselin targeted Jak2 to block the proinflammatory phenotype of macrophages, thus ameliorating inflammatory conditions.

Methods

Animals and ethical statement

Animal welfare and experimental procedures were carried out strictly in accordance with the Guide for the Care and Use of Laboratory Animals (National Institutes of Health, USA) 'The Detailed Rules and Regulations of Medical Animal Experiments Administration and Implementation' (Order No. 1998–55, Ministry of Public Health, China) and approved by the Laboratory Animal Ethics Committee of School of Life Sciences, Nanjing University. Animal studies were reported in compliance with the ARRIVE guidelines (Kilkenny *et al.*, 2010; McGrath and Lilley, 2015). All efforts were made to minimize the animals' suffering and to reduce the number of animals used.

Female C57BL/6 mice (6–8 weeks old, 18–22 g) were obtained from Model Animal Genetics Research Center of Nanjing University (Nanjing, China). They were maintained with free access to pellet food and water in plastic cages at 21 ± 2°C and kept on a 12 h light/dark cycle in specific-pathogen-free facilities.

Study design

Several animal models have been developed to mimic the typical pathophysiological change in septic patients with sepsis. Caecal ligation and puncture (CLP) in rodents has become the most widely used model and is considered to be the gold standard in sepsis research (Buras *et al.*, 2005; Rittirsch *et al.*, 2007). Mice are sensitive to sepsis and share high homology with humans. Thus, we used CLP-induced polymicrobial sepsis to evaluate the therapeutic activity of seselin in C57BL/6 mice. Mice were randomly assigned to five experimental groups (10 mice per group) after acclimatizing

to the housing environment for 7 days: (i) sham, (ii) vehicle-treated CLP, (iii) CLP mice treated with seselin (3 mg·kg^{-1}; dissolved in olive oil; in a volume of 100 μL·per 20 g), (iv) CLP mice treated with seselin (10 mg·kg^{-1}), (v) CLP mice treated with seselin (30 mg·kg^{-1}). Data collection and analysis were performed blindly, and the experimenters were unaware of the group assignment and animal treatment.

CLP surgery was performed as described previously (Rittirsch *et al*., 2008). Briefly, mice were anaesthetized with an i.p. injection of 2% sodium pentobarbital (150 μL·per 20 g) and then the lower quadrants of the abdomen were shaved. Mice were placed onto styrofoam pads and the shaved area disinfected with 75% ethanol. An incision along the abdominal midline was made carefully to expose the caecum, without exposing the remainder of the small and large bowel and avoiding damage to blood vessels. The caecum was ligated tightly with a 3–0 silk suture at the middle, between basal and distal poles to induce a 'mid-grade' sepsis. The ligated caecum was punctured through-and-through twice with a 20-gauge needle and pushed gently to expel faecal material from the punctures. The caecum was then relocated into the abdominal cavity. The abdominal incision was closed with two layers of 4–0 silk suture. Prewarmed (37°C) normal saline (1 mL) was injected to resuscitate animals immediately after the operation. For the sham group of animals, the caecum was exposed but without ligation and puncture and then returned to the abdomen. All animals received buprenorphine (0.05 mg·kg, s.c.) for postoperative analgesia and repeated every 6 h.

In survival studies, mice were given intragastrically, a range of doses of seselin or the same volume of vehicle (olive oil) 2 h prior to CLP surgery. Animals were killed by an overdose of sodium pentobarbital (300 μL·per 20 g of 2% sodium pentobarbital i.p.) if humane end points were reached (weight loss ≥20% of pre-experimental body weight). The survival was recorded for 60 h after CLP when the number was stable (no more deaths). The survivors were monitored for another 3 weeks to ensure there was no late mortalities.

Under anaesthesia, blood samples (500 μL each mice) and lung tissues were collected 4 h after CLP and stored at −80°C until further analysis.

Cells

Cultures of bone marrow-derived macrophages (BMDMs) were established as previously described (Feng *et al*., 2014). In brief, mice were killed by an overdose of sodium pentobarbital, and the femurs were flushed with PBS by a 21-gauge needle. Harvested cells (1 × 10^7 cells per well) were grown in RPMI 1640 containing 10% FBS and 10 ng·mL^{-1} macrophage-colony stimulating factor (**M-CSF**, Peprotech, Rock Hill, NJ, USA) in 5% CO_2 at 37°C for 7 days in six-well plate. Adherent macrophages (approximately 1 × 10^6 cells per well) were washed twice with PBS and cultured with fresh DMEM medium containing 10% FBS. Cultures of BMDM were stimulated with 10 ng·mL^{-1} LPS and 10 ng·mL^{-1} IFN-γ or 20 ng·mL^{-1} **IL-4** to induce the pro- or anti-inflammatory phenotype.

Murine RAW 264.7 cells, obtained from the American Type Culture Collection (Rockville, MD, USA), were cultured in DMEM (GIBCO, Grand Island, NY, USA) containing 10% FBS (GIBCO, Grand Island, NY, USA), 100 U·mL^{-1} penicillin and 100 μg·mL^{-1} streptomycin in 5% CO_2 at 37°C.

Cytokine analysis by ELISA

Blood samples were incubated at 37°C for 30 min and then centrifuged at 1500 x *g* for 15 min at 4°C. Cytokines, IL-1β, IL-6 and TNF-α, in the serum, were measured using ELISA kits from Dakewe Biotech Co. Ltd. according to the manufacturer's instructions.

Bronchoalveolar lavage fluid (BALF) and lung single-cell suspensions collection and analysis

Four hours after CLP surgery, anaesthetized mice were heparinised with 1% heparin (100 μL per·20 g, i.p.) and then killed with an overdose of sodium pentobarbital. Blood (0.5mL) was collected. The chest was opened and the trachea exposed carefully. We made a small incision at the top of trachea with a needle to insert an 18-gauge catheter, which was secured tightly with 3-0 silk suture. Bronchoalveolar lavage (BAL) was performed by three times with PBS (0.5 mL). The recovery of the fluid was about 90%. BALF was centrifuged 1500 x *g* for 10 min at 4°C. Cytokines, **IL-1β**, **IL-6** and **TNF-α**, in the supernatants of BALF, were measured using commercial ELISA kits. After filtering through 40 μm nylon mesh, cells was re-suspended in PBS to count total cell number with a haemocytometer and the profile of immune cell subsets analysed with flow cytometry.

Lung single-cell suspensions were prepared as described previously (Yu *et al*., 2016). Briefly, after BALF was harvested, the thorax was opened, the left atrium nicked and the lungs perfused with PBS through the right atrium to remove the blood. A small incision was made on the top of trachea, and an 18 gauge angiocath was inserted and secured. The lungs were then inflated through the tracheal catheter with 1 mL digestion solution containing 1.5 mg·mL^{-1} of collagenase A (Roche) and 0.4 mg·mL^{-1} DNase I (Roche) in HBSS plus 0.5% FBS and 10 mM HEPES. After tying off the trachea, The heart and mediastinal tissues were carefully removed, the lungs were excised and incubated in 5 mL digestion solution at 37°C for 30 min, with gentle vortexing every 8–10 minutes. At the end of the digestion (30 min), we added 25 mL PBS and then cut the lung tissue into small pieces. The suspension of lung tissue was then filtered through 40 μm nylon mesh and the filtrate (a suspension of single cells) treated with Tris-NH_4Cl solution to lyse erythrocytes. The immune cells in the cell suspension were analysed by flow cytometry, as described below.

Cells from BALF and lung tissue were analysed on a SORP FACSARIA II cytometer (BD Biosciences, San Jose, CA, USA). Antibodies for **CD11b**-PE (clone M1/70, Cat # 12-0112-81), F4/80 PE-Cyanine7 (clone BM8, Cat # 25-4801-82), Ly-6G APC (clone 1A8-Ly6g, Cat # 17-9668-82) and Ly-6C PerCP-Cyanine5.5 (clone HK1.4, Cat # 45-5932-82) were purchased from ThermoFisher Scientific. Antibodies for **CD45** APC/Fire™ 750 (clone 30-F11, Cat # 103153) and **CD11c**-FITC (clone N418, Cat # 117306) were purchased from Biolegend (San Diego, CA, USA). Cells collected from BALF and lung tissue were first suspended in 0.4% Trypan blue to ensure viability was more than 95%. The cells were incubated with anti-CD45, anti-F4/80, anti-CD11c, anti-CD11b, anti-

Ly6G and anti-Ly6C for 30 min at 4°C in dark and then by flow cytometry for immunophenotypic analysis. In BALF, $CD45^+$ cells were gated to further analyse the $F4/80^+CD11c^+$ alveolar macrophages, $CD11b^+Ly6G^+$ neutrophils and $CD11b^+Ly6C^+$ monocytes. Lung single-cell suspensions were prepared from lavaged lung (from which the BALF was harvested) to reduce contamination by alveolar macrophages. Similarly, $CD45^+$ cells were gated to further analyse the $F4/80^+CD11c^+$ interstitial macrophages and the $CD11b^+Ly6C^+$ monocytes. $CD11b^+Ly6G^+$ neutrophils were distinguished from all other leukocytes. Isotype antibodies (APC/Fire™ 750 Armenian Hamster IgG clone HTK888 for **CD4**, FITC Armenian Hamster IgG clone HTK888 for FITC, Rat IgG2c, κ clone RTK4174 for Ly-6C were purchased from Biolegend; Rat IgG2b κ Isotype-PE Cat # 12-4031-82 for CD11b, Rat IgG2a κ Isotype-PE-Cyanine7 Cat # 25-4321-82 for F4/80, Rat IgG2a κ Isotype-APC Cat # 17–4321-81 for Ly-6G were purchased from ThermoFisher Scientific) were used to determine non-specific binding.

Immunohistochemistry (IHC) and immunofluorescence assay

Lung tissue was fixed with formalin immediately and then embedded in paraffin. Paraffin-embedded lung sections were heat-fixed, deparaffinized, rehydrated, antigen retrieval, blocked with 3% goat serum and stained with H&E to observe tissue morphology, or incubated with anti-CD11c (Cat # ab52632, Abcam) overnight at 4°C. The slides were examined using Real Envision Detection kit (GeneTech, Shanghai, China) according to the manufacturer's instructions. Other lung sections were incubated with PE-CD11b overnight at 4°C and then observed with a confocal laser scanning microscope (Olympus, Lake Success, NY, USA).

MTT assay

Cells were seeded in 96-well plate and incubated with various concentrations of compounds, with or without LPS and IFN-γ or IL-4 for 24 h. Then MTT (20 μL of 4 $mg{\cdot}mL^{-1}$ MTT dissolved in PBS) was added to each well and incubated at 37°C for 4 h. The plate was centrifuged at 1200× *g* for 5 min and the supernatant discarded. DMSO (200 μL) was added to each well and the plate shaken for 10 min. The absorbance at 570 nm was measured.

Carboxyfluorescein diacetate succinimidyl ester (CFSE) assay

Cell proliferation was determined by CFSE assay according to the manufacturer's instructions. CFSE (Cat # C34554) was purchased from ThermoFisher Scientific. Briefly, stock solutions of CFSE were prepared at a concentration of 5 mM or 100 mM in 100% DMSO and the diluted with pre-warmed (37°C) FBS-free DMEM medium to 2 μM. RAW 264.7 cells were cultured to the desired density and incubated with the 2 μM CFSE solution for 30 min at 37°C. The CFSE solution was removed and the cells washed twice before replacing with fresh, pre-warmed complete culture medium. Labelled cells were incubated with various doses of compounds in the presence of LPS and IFN-γ or IL-4 for 24 h. Cell proliferation was assessed by flow cytometry.

Quantitative PCR

Total RNA were extracted from cells or tissues and reverse transcribed to cDNA and subjected to quantitative PCR, which was performed with the BioRad CFX96 Touch™ Real-Time PCR Detection System (BioRad, CA, USA), and threshold cycle numbers were obtained using BioRad CFX manager software. The program for amplification was one cycle of 95°C for 2 min followed by 40 cycles of 95°C for 10 s and 60°C for 30 s. The primer sequences used in this study were as follows: *mIl-1β*, 5′-CTTCAGGCAGGCAGTATCACTC-3′ (forward) and 5′-TGCAGTTGTCTAATGGGAACGT-3′ (reverse); *mIl-6*, 5′-ACAACCACGGCCTTCCCTAC-3′ (forward) and 5′-TCTCATTTCCACGATTTCCCAG-3′ (reverse); *mTnf-α*, 5′-CGAGTGACAAGCCTGTAGCCC-3′ (forward) and 5′-GTCTTTGAGATCCATGCCGTTG-3′ (reverse); *mIl-23*, 5′-ATGCTGGATTGCAGAGCAGTA-3′ (forward) and 5′-ACGGGGCACATTATTTTTAGTCT-3′ (reverse); *mIl-12*, 5′-TGAGCAGGATGGAGAATTACAGG-3′ (forward) and 5′-GTCCAAGTTCATCTTCTAGGCAC-3′ (reverse); *mCcl3*, 5′-TGAGAGTCTTGGAGGCAGCGA-3′ (forward) and 5′-TGTGGCTACTTGGCAGCAAACA-3′ (reverse); *mCcl7*, 5′-TTGTGTTCGCCTGTAGTGCATA-3′ (forward) and 5′-CAGGAAGTTGGTGAGCTGGTATA-3′ (reverse); *mCxcl11*, 5′-GGCTTCCTTATGTTCAAACAGGG-3′ (forward) and 5′-GCCGTTACTCGGGTAAATTACA-3′ (reverse); *mFizz1*, 5′-AGGAGCTGTCATTAGGGACATC-3′ (forward) and 5′-GGATGCCAACTTTGAATAGG-3′ (reverse); *mYm1*, 5′-AGAAGGGAGTTTCAAACCTGGT-3′ (forward) and 5′-GTCTTGCTCATGTGTGTAAGTGA-3′ (reverse); *mArg-1* 5′-CTCCAAGCCAAAGTCCTTAGAG-3′ (forward) and 5′-AGGAGCTGTCATTAGGGACATC-3′ (reverse); *mCcl22* 5′- AGGTCCCTATGGTGCCAATGT-3′ (forward) and 5′-CGGCAGGATTTTGAGGTCCA-3′ (reverse); *mCd163* 5′-ATGGGTGGACACAGAATGGTT-3′ (forward) and 5′-CAGGAGCGTTAGTGACAGCAG-3′ (reverse); *mβ-actin*, 5′-TGCTGTCCCTGTATGCCTCT-3′ (forward) and 5′-TTTGATGTCACGCACGATTT-3′ (reverse). *hIL-6*, 5′-ACTCACCTCTTCAGAACGAATTG-3′ (forward) and 5′-CCATCTTTGGAAGGTTCAGGTTG-3′ (reverse); *hTNF-α*, 5′-TCTCTAATCAGCCCTCTGGCC-3′ (forward) and 5′-TGGGCTACAGGCTTGTCACTC-3′ (reverse); *hβ-ACTIN*, 5′-TGTGATGGTGGGAATGGGTCAG-3′ (forward) and 5′-TTTGATGTCACGCACGATTTCC-3′ (reverse). The relative amount of each gene was normalized to the amount of *β-actin* and then reported as fold change of basal level.

Western blots

Collected cells were lysed in lysis buffer; and the lysates were separated by 10% SDS-PAGE and electrophoretically transferred onto PVDF membranes (Millipore Corp., Bedford, MA, USA). The membranes were blocked with 3% BSA for 1 h at room temperature, probed with indicated primary antibodies overnight at 4°C and then incubated with a HRP coupled secondary antibody. Protein bands were visualized using Western blotting detection system, according to the manufacturer's instructions.

Flow cytometry analysis for activated BMDMs

Cultured cells were harvested and washed twice with cold PBS. Collected cells were stained with specific antibodies for 30 min at 4°C in dark and analysed by flow cytometry.

Phagocytosis assays were conducted using fluorescent red latex beads (1 μm diameter, L-2778, Sigma-Aldrich). Latex beads were opsonized with complete medium (10% FBS in BMDM) for 30 min at 37°C before the experiments. Opsonized beads were added to seselin-treated cells at a ratio of 10:1 (beads : cells) and incubated at 37°C for 2 h. Phagocytosis was stopped by washing and addition of 1 mL ice-cold sterile PBS. Cells were harvested and washed in ice-cold PBS three times and then analysed by flow cytometry.

Confocal microscopy

Cells were washed with cold PBS, fixed in Lyse/fix buffer (diluted by PBS, BD PharMingen) for 30 min, permeabilized with 0.5% Triton X-100 for 30 min and blocked with 3% BSA for 1 h. Then cells were stained with anti-STAT1 or anti-p65 overnight at 4°C and then with specific fluorescent-coupled secondary antibody for 2 h. The coverslips were counterstained with DAPI and imaged with a confocal laser scanning microscope (Olympus, Lake Success, NY, USA).

Quantification of immunofluorescence and immunohistochemistry assay

The quantification of CD11b, F4/80, CD11c positive cells in lung tissue and STAT1, p65 location in RAW 264.7 cells was performed by ImageJ software (https://imagej.nih.gov/ij/).

For the quantification of STAT1 and p65 location (as in Figure 4G, H), STAT1/p65 and the corresponding DAPI single staining images in the same field of view were opened in ImageJ and converted to grey type (Image-Type-8 bit). The converted images were stacked into one window (Image-Stacks-Images to stack). We draw a line using the 'Straight' in toolbar in one of the images, which will appear at the same location on the other image. We marked the two ends of the line as 'α' and 'ω' respectively. We analysed the grayscale value from 'α' to 'ω' in both STAT1/p65 and the corresponding DAPI single staining images (Analyse-Plot profile). Mean fluorescence intensity was presented as the means of plot values and normalized in arbitrary units.

For the quantification of CD11b positive cell numbers in lung tissue in Figure 6A, images were also converted to grey type and the colour of background and the particles inverted (Edit-Invert), to make the background white and particles black. We adjusted brightness/contrast (Image-Adjust-Brightness/Contrast-Auto-Apply) and threshold (Image-Threshold-Auto-Apply). Then we analysed the positive cell numbers *via* Analyse-Analyse particles. Acquired data were expressed as means ± SEM of five fields per mouse in every group.

The quantification of CD11c positive cell numbers in lung tissue in Figure 6C was performed using plugins called IHC Toolbox download. We opened the images in ImageJ and clicked IHC Tool box, started training process by selecting representative area as region of interest using 'Rectangle' bottom in Toolbar and then adjusted the Colour chooser to ensure that all positive area was selected. We converted the newly generated images into 8-bit and then analysed the positive areas *via* Analyse-Measure after we checked the 'Limited to threshold' (Analyse-Set measurements). Acquired data were normalized to the amount of the CLP-treated group.

Co-immunoprecipitation (co-IP)

RAW 264.7 cells were cultured in 10 mm dishes and pretreated with seselin in the presence of LPS and IFN-γ. The control group receieved the same volume of DMSO. The lysates of the harvested cells were incubated with 2 μg appropriate antibody at 4°C overnight and precipitated with protein A/G-agarose beads (Santa Cruz, Cat # sc-2003) for another 4 h at 4°C. The beads were washed with lysis buffer four times by centrifugation at 1000× *g* for 5 min at 4°C, and the immunoprecipitated proteins were analysed by Western blot.

Cellular thermal shift assay (CETSA)

CETSA was performed as described previously reported (Jafari *et al.*, 2014). Briefly, cultured cells were incubated with 20 μM seselin or the same volume of DMSO for 2 h. Harvested cells were equally divided and lysed using three cycles of freeze-thawing with liquid nitrogen and then heating with various temperatures with a PCR instrument respectively, centrifuging at 20 000× *g* for 20 min at 4°C in order to separate the soluble fractions from precipitates. The supernatants were transferred to new microtubes and analysed by Western blot.

Macrophage depletion and BMDM adoptive transfer and LPS induced sepsis

Systemic macrophages were depleted by i.p. administration of **clodronate** liposome to mice (100 μL·per 20 g body weight). Twenty-four hours later, the proportion of CD11b positive macrophage populations in the peritoneal cavity was analysed by flow cytometry. BMDM was polarized to the proinflammatory phenotype with 10 ng·mL^{-1} LPS and 10 ng·mL^{-1} IFN-γ and treated with 20 μM seselin or the same volume of DMSO for 6 h. Normal BMDM (M0-BMDM) received the same volume of DMSO. The pretreated cells were harvested and washed three times with cold PBS and then transferred to the macrophage-depleted mice (1×10^6 cells per 20 g ; 100 μL per mouse, i.v.) 2 h before LPS challenge.

C57BL/6 mice were injected with LPS (i.p.; 10 mg·kg^{-1}) and survival was monitored. Animals were killed by an overdose of sodium pentobarbital (2% sodium pentobarbital, 300 μL·per 20 g; i.p.) if humane end points were reached (weight loss ≥20% of pre-experimental body weight). The survival was recorded for 60 h, when there were no more deaths. The survivors were monitored for another 3 weeks to make sure there was no late mortalities.

Under anaesthesia, blood samples were collected 4 h after LPS challenge (the peak point).

Data and statistical analysis

The data and statistical analysis comply with the recommendations on experimental design and analysis in pharmacology (Curtis *et al.*, 2018). All experiments were randomized and blinded. Results from MTT and QPCR were expressed as mean ± SEM of five independent experiments with each experiment including triplicate sets. Results from Western blot and flow cytometry were represented as mean ± SEM of five independent experiments. Data from CETSA were normalized.

Statistical analysis was performed with GraphPad Prism 5.0 software (San Diego, CA, USA). Student's *t*-test was used to determine the significance of difference between two

groups. One-way ANOVA analysis followed by Dunnett's *post hoc* test was used to evaluate the differences between various experimental when there were more than two groups. Post tests were run only if F achieved $P < 0.05$. The level of significance was set at a P value of 0.05. LPS and IFN-γ or LPS followed by ATP treatment was set as control for *in vitro* experiments; CLP or LPS treatment was set as control for *in vivo* experiments.

Materials

Seselin (chemical structure shown in Figure 1A; from Toronto Research Chemicals, North York, Canada) was dissolved at a concentration of 20 mM or 100 mM in 100% DMSO as a stock solution, stored at −20°C and diluted with medium before each experiment. LPS, 3-(4,5-dimethyl-2-thiazyl)-2,5-diphenyl-2*H*-tetrazolium bromide (MTT), latex beads (amine-modified polystyrene, fluorescent red), DAPI, phorbol 12-myristate 13-acetate (PMA), sodium pentobarbital and tofacitinib were purchased from Sigma-Aldrich (St. Louis, MO, USA). Recombinant murine IFN-γ (Cat # 315-05), IL-4 (Cat # 214-14) and M-CSF (Cat # 315-02) and recombinant human IFN-γ (Cat # 300-02) were purchased from Peprotech (Rocky Hill, NJ, USA). Antibodies for p-STAT1 (Cat # 9167), STAT1 (Cat # 9172), p-p65 (Cat # 3033), p65 (Cat # 8242), p-Jak2 (Cat # 3771), Jak2 (Cat # 3230), TLR4 (Cat # 14358), p-IKKα/β (Cat # 2697) and **IKK** (Cat # 2682) were purchased from Cell Signaling Technology (Beverly, MA, USA). Anti-caspase1 (Cat # ab108362) and anti-CD11c (Cat # ab52632, used in immunohistochemistry) were purchased from Abcam (Burlingame, CA, USA). Anti-**IFNγR1** (Cat # YT2280) was purchased from Immunoway (Plano, TX, USA). Anti-tubulin (Cat # M20005) and actin (Cat # M20011) were purchased from Abmart (Shanghai, China). PE-anti-**inducible NO synthase (iNOS)** (Cat # 12–5920-82) and PE Rat IgG2a κ Isotype Control (Cat # 12-4321-81) were purchased from ThermoFisher Scientific (Waltham, MA, USA). Goat anti-Rabbit IgG (H + L) Secondary Antibody, Alexa Fluor 594 and Goat anti-Rabbit IgG (H + L) Secondary Antibody, Alexa Fluor 488 were purchased from ThermoFisher Scientific. ELISA kit for murine IL-1β, IL-6 and TNF-α was purchased from Dakewe Biotech Co. Ltd. (Shenzhen, China). Clodronate liposome and PBS liposome were purchased from clodronateliposomes.com. All other chemicals were purchased from Sigma Chemical Co.

Nomenclature of targets and ligands

Key protein targets and ligands in this article are hyperlinked to corresponding entries in http://www.guidetopharmacology.org, the common portal for data from the IUPHAR/BPS Guide to PHARMACOLOGY (Harding

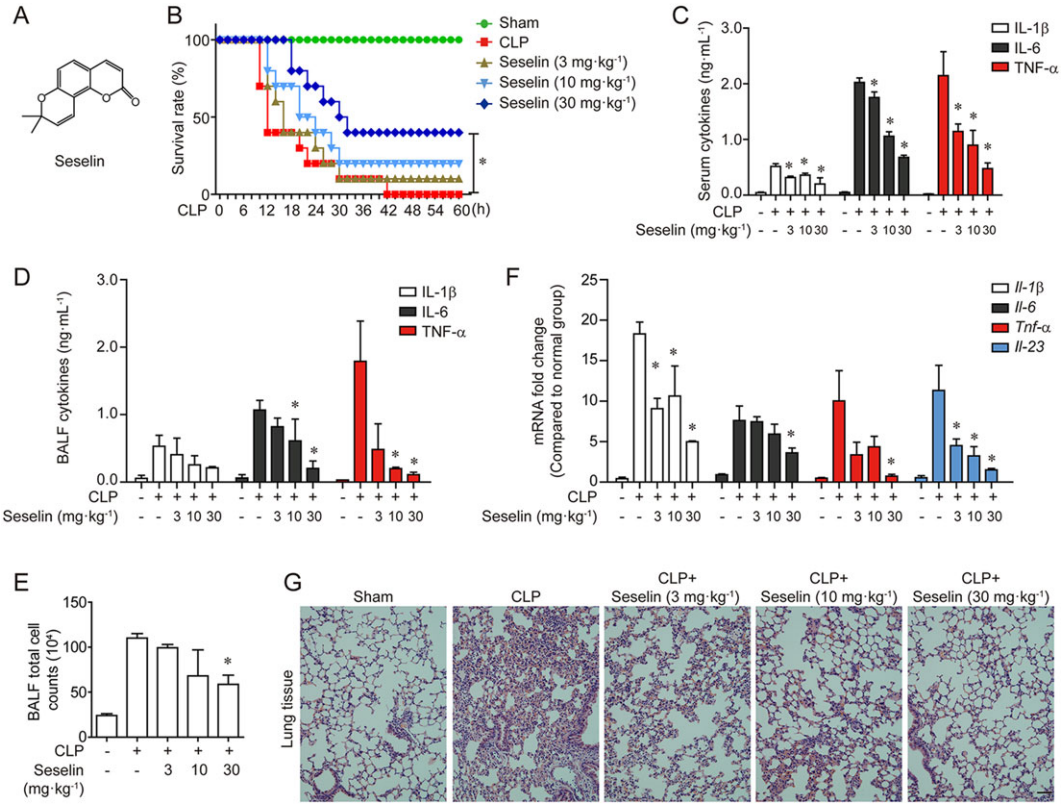

Figure 1

Seselin ameliorated CLP-induced sepsis in mice. (A) Structure of seselin. (B) Various doses of seselin or vehicle (olive oil) given intragastrically 2 h before CLP surgery. Survival rate was observed and calculated (n = 10 mice per group). Mice were treated as (B). Four hours later, cytokines in serum (C) and BALF (D) were determined by ELISA. (E) Total cell numbers in BALF were determined. (F) mRNA level of cytokines in lung tissue was determined by QPCR. (G) Haematoxylin and eosin staining of lung sections. Scale bar 50 μm. *$P < 0.05$, significantly different from CLP group.

et al., 2018), and are permanently archived in the Concise Guide to PHARMACOLOGY 2017/18 (Alexander *et al.*, 2017a, b, c).

Results

Seselin ameliorated disease progress and lung damage of CLP induced sepsis in mice

To evaluate the therapeutic potential of seselin in inflammatory conditions, we performed CLP to induce sepsis in mice and treated them with seselin (3-30 mg kg^{-1}). Results from Figure 1B, C showed that seselin administration significantly improved survival rate and suppressed systemic levels of proinflammatory cytokines (IL-1β, IL-6 and TNF-α). As the lung is a major site of damage during the pathogenesis of sepsis, we assessed if seselin protected lung tissue from damage. Proinflammatory cytokines (IL-1β, IL-6 and TNF-α) and infiltrated cells in BALF was significantly decreased (Figure 1D, E), as well as the mRNA levels for these cytokines in lung tissue (Figure 1F), after treatment with seselin. Histological analysis of the lung tissue from CLP mice confirmed infiltration of leukocyte cells and demonstrated excessive interstitial and intra-alveolar oedema. Compared to the model (CLP only) group, administration of seselin clearly ameliorated the lung damage induced by CLP (Figure 1G). These observations showed that seselin exerted anti-inflammatory activity *in vivo*.

Seselin decreased the proinflammatory phenotype of macrophages, dose- and time-dependently

As macrophages play an essential role during sepsis, we evaluated the anti-inflammatory activity of seselin on cultures of BMDMs. We first performed MTT assays to test cytotoxicity of seselin. Data in Supporting Information Figure S1A–C showed that seselin showed very little cytotoxicity, even at a high concentration (80 μM), on normal, unstimulated BMDMs or those stimulated with LPS and IFN-γ or IL-4. . In addition, the proliferation of macrophages, assessed by CFSE staining, was also unaffected by seselin treatment (Supporting Information Figure S1D). However, seselin reduced the mRNA for cytokines (*Il-1β*, *Il-6*, *Tnf-α* and *Il-23*) and chemokines (*Ccl3*, *Ccl7*, *Cxcl9* and *Cxcl11*) concentration-dependently in BMDMs stimulated with LPS and IFN-γ (Figure 2A–D and Supporting Information Figure S2A). Consistent with these data, the ELISA assay results (Figure 2E) demonstrated that seselin reduced the IL-6 and TNF-α protein secreted into the cell supernatants. The cytokine IL-1β is an important component of the inflammatory response and its secretion requires both the activation of the NF-κB signal, primed by LPS, and the assembly of an inflammasome, induced by ATP. In BMDM cultures stimulated with LPS and then exposed to ATP, both IL-1β and TNF-α secretion was increased, and seselin markedly suppressed expression of the cytokines (Figure 2F). In addition, BMDMs were polarized to the proinflammatory phenotype for various time points and peaked at 3–6 h after stimulation. Seselin also suppressed the mRNA levels for *Il-1β*, *Il-6* and *Tnf-α* during this procedure in a time dependent manner (Figure 2G).

In the classical activation of macrophages (LPS and IFNγ), iNOS is a key enzyme of NO production. When BMDMs were treated with seselin, the expression of iNOS was significantly down-regulated, compared with that in the classically activated macrophages (Figure 3A). One of the characteristics of macrophages, phagocytosis, is substantially increased when these cells are polarized to the proinflammatory phenotype. We assayed phagocytosis by the uptake of red fluorescent linked beads and showed it to be greatly increased in macrophages activated by LPS and IFN-γ and that seselin reduced this increase (Figure 3B). Another marker expressed on the cell surface of classically activated macrophages is CD11c and incubation with seselin clearly decreased the percentage of CD11c positive BMDMs, concentration-dependently (Figure 3C). Pretreatment with IL-4 did not increase any of these three markers in BMDMs and seselin also did not affect these markers in IL-4 pretreated macrophages (Supporting Information Figure S2B). Taken together these data show that seselin suppressed the proinflammatory aspects of BMDMs.

Seselin blocked the STAT1 signalling pathway

To elucidate the mechanism(s) by which seselin suppressed the inflammatory responses of macrophages, the major signalling pathways involved - Jak2-STAT1 and NF-κB - were investigated. Seselin treatment suppressed expression of p-STAT1 and p-p65 (a critical component of NF-kB signalling), both concentration and time dependently (Figure 4A–D). As transcription factors, STAT1 and p65 need to be translocated to the nucleus to mediate the expression of relevant genes. To confirm the effects of seselin on STAT1 and p65, we used immunofluorescent assays to localise the intracellular site of these transcription factors. Stimulation of BMDMs with LPS and IFN-γ induced accumulation of STAT1 and p65 in the nucleus, as indicated by merging with DAPI. Consistent with the results obtained in the Western blots (Figure 4A), seselin inhibited the amount of STAT1 located in nucleus, indicating its decreased transcriptional activity (Figure 4G). p65 was also mainly located in the cytoplasm in seselin-treated cells, compared with the model group (Figure 4H). We also used the inflammasome model (LPS +ATP) in BMDMs to analyse the down-regulated release of IL-1β by seselin. As shown in Figure 4E, F, seselin reduced both the level of p-p65 and cleaved-caspase 1, p10 and p20, the activated form of caspase 1. However, seselin had much less effect on upstream proteins, including TLR4 expression and IKKα phosphorylation (Figure 5A). These data indicated critical role for STAT1 and p65 signalling pathways in the seselin-mediated inhibition of the proinflammatory phenotype of macrophages. However, as shown in Figure 5A, seselin produced a greater inhibition of STAT1 than of p65.

Seselin targeted Jak2 to block its activity

To investigate how seselin inhibited the activation of macrophages, we used co-IP to detect the interaction between key upstream signal proteins. As shown by Western blots, seselin clearly decreased the interaction between Jak2 and IFN-γR, as well as the interaction with STAT1, consistent with a reduced activation of Jak2 and STAT1 (Figure 5A). These observations suggested that Jak2 might be a candidate target of seselin. To

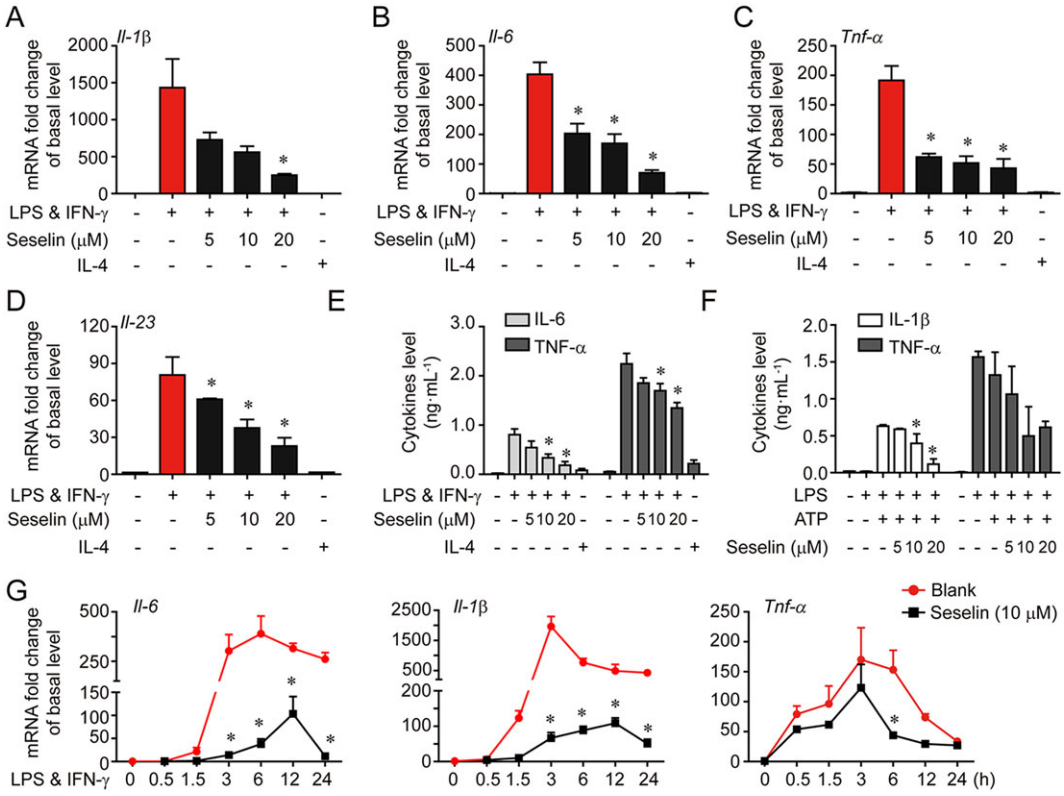

Figure 2

Inhibition by seselin of cytokine output from macrophages stimulated by LPS and IFN-γ. BMDM were incubated with various doses of seselin or the same volume of DMSO in the presence of 10 ng·mL^{-1} LPS and 10 ng·mL^{-1} IFN- γ, or 20 ng·mL^{-1} IL-4, for 6 h. The mRNA levels of *Il-1β* (A), *Il-6* (B), *Tnf-α* (C) and *Il-23* (D) were determined by quantitative PCR. (E) Secreted IL-6 and TNF-α in supernatant was measured by ELISA. *$P < 0.05$, significantly different from LPS and IFN-γ treated group. (F) BMDMs were incubated with various doses of seselin or the same volume of DMSO in the presence of 10 ng·mL^{-1} LPS for 3 h, followed by 5 mM ATP for 1 h. IL-1β and TNF-α in the supernatants was measured by ELISA. *$P < 0.05$, significantly different from LPS and ATP treated group. (G) BMDMs were incubated with 10 μM seselin or the same volume of DMSO in the presence of 10 ng·mL^{-1} LPS and 10 ng·mL^{-1} IFN-γ for various time points. The mRNA levels of *Il-1β*, *Il-6* and *Tnf-α* were determined by quantitative PCR. *$P < 0.05$, significantly different from LPS and IFN-γ treated group at the same time point. Data are represented as mean ± SEM of five independent experiments.

test this hypothesis, we performed CETSA to confirm the interaction between seselin and Jak2. As shown in Figure 5B, seselin enhanced the thermal stability of Jak2 at higher temperatures, compared to DMSO treatment (Figure 5B, C). At a constant time of heating and temperature, seselin protective effects on Jak2 protein were concentration-dependent protection on Jak2 protein level (Figure 5D, E). We then used molecular docking analysis to investigate possible binding mode of seselin with the crystal structures of Jak2 (31-516aa) (PDB ID: 4Z32). Docking results in Figure 5F predicted that seselin might form hydrogen binds with His82 and Glu65, the FERM domain of Jak2. In addition, the pyran ring and phenyl ring could form π–π interactions with Cys68 and Pro389, which are also located in the FERM domain, responsible for associating with IFN-γR. We also analysed the interaction between seselin with other function domains of Jak2. The binding energy between seselin and 840–1132 aa of Jak2 (PDB ID: 3UGC), the kinase domain, was comparable to 31-516aa, mainly *via* van der Waals forces with similar residues to tofacitinib, but no hydrogen bond was observed (Figure 5G, H). Collectively, these results suggested that seselin targeted Jak2 to block the upstream section of the STAT1 signalling pathway.

Protection by seselin of septic mice was due to its inhibition of the macrophage proinflammatory phenotype

To confirm these mechanisms *in vivo*, we next determined the effects of seselin on macrophages isolated from lung tissue taken from mice after CLP. Results of staining for CD11b showed a significantly mitigated infiltration of immune cells in lung tissue from seselin treated mice, compared with values in the CLP only (model) group. This inhibition was dose-dependent (Figure 6A, C). Immunohistochemical assay revealed decreased level of CD11c expression, suggesting a decrease in the infiltrating proinflammatory macrophages in lung tissue (Figure 6B, D). Consistent with previous data, seselin also inhibited the levels of p-Jak2, p-STAT1 and p-p65 in lung tissue from CLP mice (Figure 6E, F). To further detected the dynamic profile of monocytes, neutrophil and the immunophenotype of macrophages, we performed flow

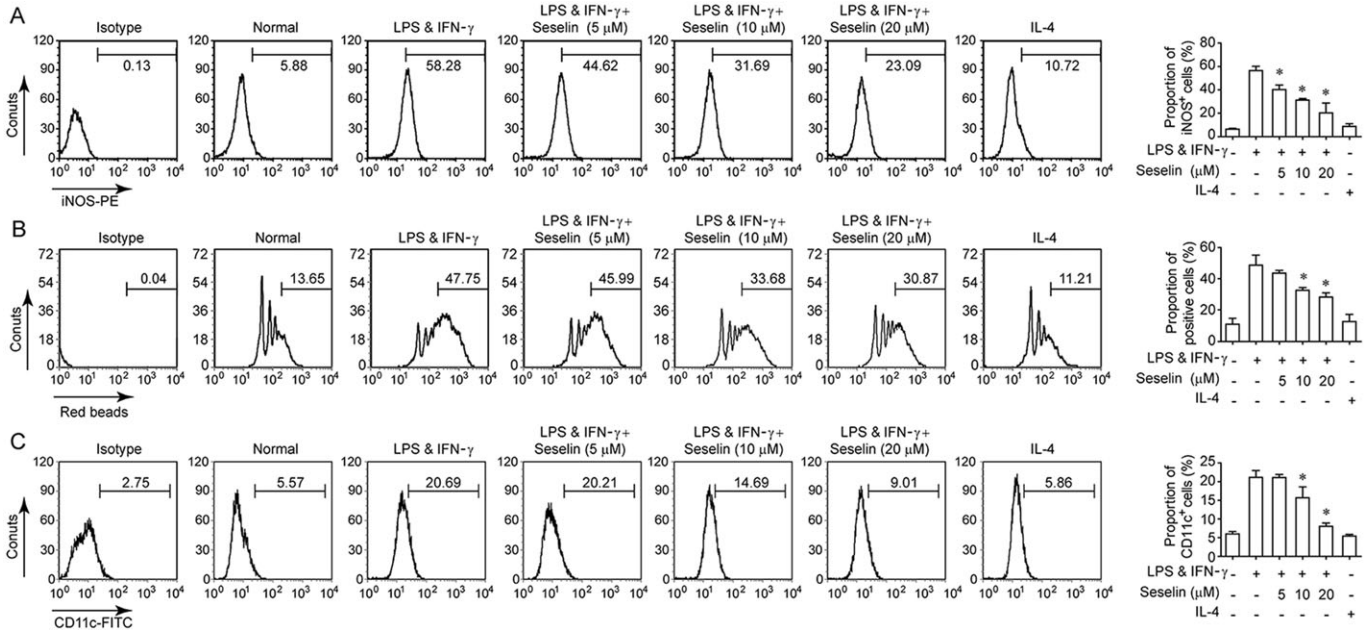

Figure 3

Seselin inhibited the expression of proinflammatory macrophage markers. BMDMs were incubated with various doses of seselin or the same volume of DMSO in the presence of 10 ng·mL^{-1} LPS and 10 ng·mL^{-1} IFN-γ, or 20 ng·mL^{-1} IL4, for 12 h. Expression of iNOS (A), phagocytosis (B) and CD11c (C) was measured by flow cytometry. The positive cells of five different experiments are shown as means ± SEM. *$P < 0.05$, significantly different from LPS and IFN-γ treated group.

cytometry analysis on cells isolated from both BALF and lung tissue. As reported, the majority of alveolar macrophages in BALF displayed an M1-like phenotype with F4/80$^+$CD11c$^+$, which was increased in CLP mice (Figure 7A). Seselin treatment significantly down-regulated both the proportion of F4/80$^+$CD11c$^+$ and the total number of alveolar macrophages (Figure 7A, B). Similarly, F4/80$^+$CD11c$^-$ interstitial macrophages were also polarized to F4/80$^+$CD11c$^+$ in CLP induced septic mice (Supporting Information Figure S3A). Meanwhile, the effects of seselin on interstitial macrophages was consistent with previous data, showing a decrease in the F4/80$^+$CD11c$^+$ proportion and in the total number of macrophages (Supporting Information Figure S3A). CLP also induced a rapid expansion and infiltration of monocytes (CD11b$^+$Ly6C$^+$) and neutrophils (CD11b$^+$Ly6G$^+$) in lung tissue (Figure 7C–F and Supporting Information Figure S3B–C). Seselin treated mice exhibited a significant decrease of monocytes but only part remission of neutrophils (Figure 7C–F and Supporting Information Figure S3B–C). In further experiments, we stimulated THP-1 cells, a human monocyte cell line, with PMA and monitored the effect of seselin on the differentiation from monocytes to macrophages. Data in Supporting Information Figure S4A–B indicated that seselin slightly inhibited the expression of CD14, the marker of THP-1 differentiation (Schwende *et al.*, 1996; Aldo *et al.*, 2013). However, the proinflammatory cytokines expressed by THP-1 derived macrophages were significantly suppressed in the seselin treated group (Supporting Information Figure S4C). All these data suggested that seselin skewed the proinflammatory phenotype of both alveolar and interstitial macrophages in septic mice.

To confirm the identity of the target cells *in vivo*, we depleted mice of macrophages with clodronate liposomes and then challenged with LPS to establish an endotoxin induced peritonitis model. As shown in Figure 6A, mice injected with PBS liposome showed a high level of CD11b positive cells which were depleted after clodronate liposome treatment (Figure 8A, B). Then, we carried out adoptive transfer of pretreated BMDMs, to these depleted mice. As shown in Figure 8C, the proinflammatory phenotypic BMDMs further decreased the survival rate of LPS-challenged mice, whereas the proinflammatory phenotypic BMDMs which had been pretreated with seselin improved survival. In addition, the proinflammatory cytokines (IL-6 and TNF-α) induced by the proinflammatory phenotypic BMDM, were dramatically reduced in mice receiving seselin-exposed proinflammatory phenotypic BMDMs (Figure 7D). These data, taken in combination with the results from cell models, suggested that the anti-inflammatory effects of seselin *in vivo* reflected its inhibition of the proinflammatory properties of macrophages.

Discussion

There is much evidence of the diversity of possible therapeutic activities of natural products (Vera *et al.*, 2011; Feng *et al.*, 2014). Coumarins are widespread and structurally multiple compounds and they display a wide range of pharmacological activities such as anti-coagulant, anti-neurodegenerative (Anand *et al.*, 2012; Gomez-Outes *et al.*, 2012), antioxidant (Kostova *et al.*, 2011), anti-cancer (Riveiro *et al.*, 2010) and anti-inflammatory (Grover and Jachak, 2015; Xu *et al.*,

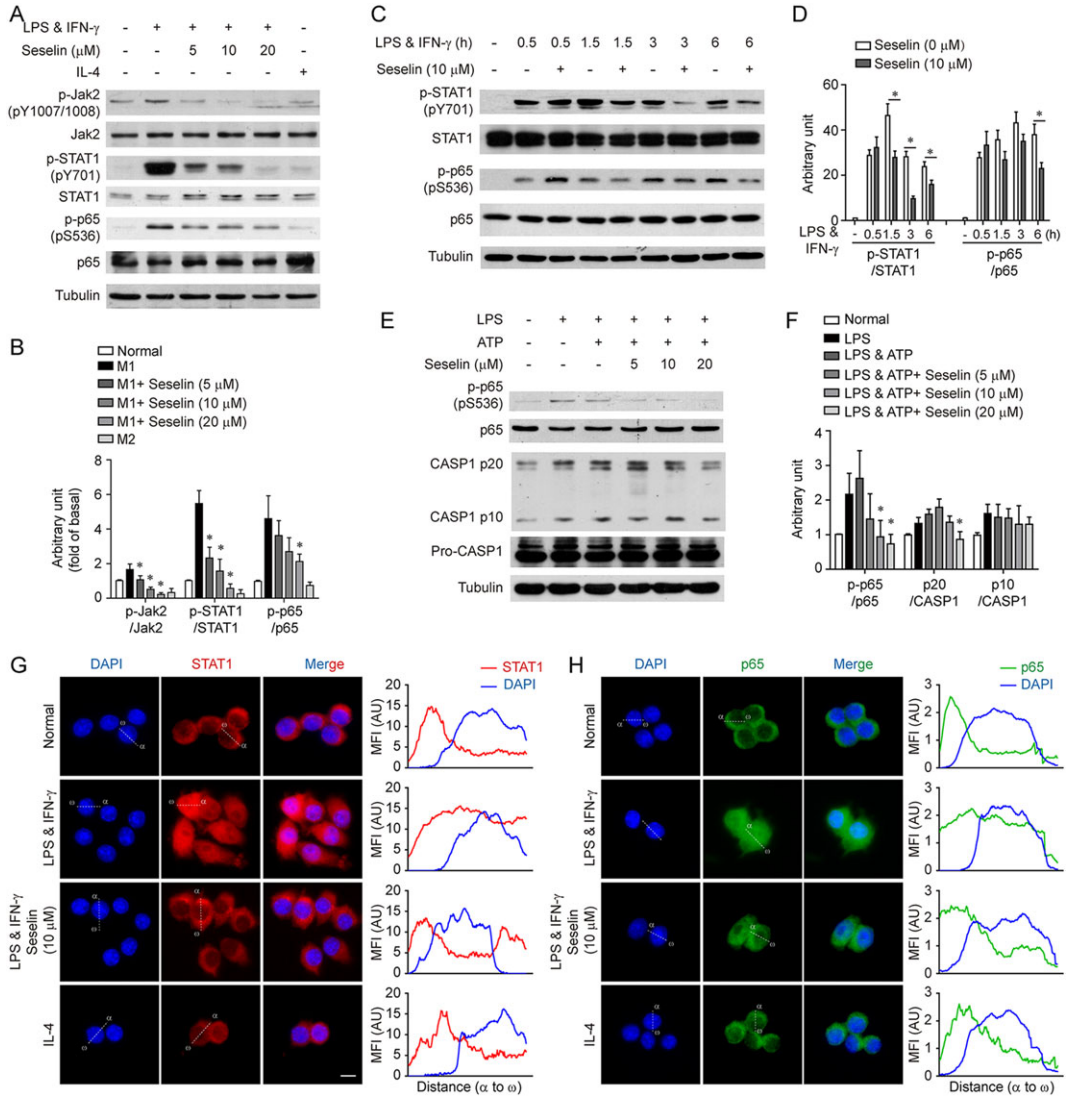

Figure 4

Seselin blocked signalling pathways that mediate the classical activation of macrophages. (A) BMDMs were incubated with various doses of seselin or the same volume of DMSO in the presence of 10 ng·mL^{-1} LPS and 10 ng·mL^{-1} IFN-γ for 6 h. Expression of p-Jak2, Jak2, p-STAT1, STAT1, p-p65, p65 and tubulin was determined by Western blot. Tubulin was a loading control. (B) Data summary of (A) is shown as means ± SEM of five independent experiments. *$P < 0.05$, significantly different from LPS and IFN-γ treated group. (C) BMDMs were incubated with 10 μM seselin or the same volume of DMSO in the presence of 10 ng·mL^{-1} LPS and 10 ng·mL^{-1} IFN-γ for various time points. p-STAT1, STAT1, p-p65, p65 and tubulin was determined by Western blot. (D) Data summary of (C) is shown as means ± SEM of five independent experiments. *$P < 0.05$, significantly different from LPS and IFN-γ treated group at the same time point. (E) BMDMs were incubated with various doses of seselin or the same volume of DMSO in the presence of 10 ng·mL^{-1} LPS for 3 h, followed by 5 mM ATP for 1 h. p-p65, p65, cleaved-caspase1 p10, cleaved caspase 1 p20, pro-caspase1 and tubulin were determined by Western blot. (F) Data summary of (E) is shown as means ± SEM of five independent experiments. *$P < 0.05$, significantly different from LPS and ATP treated group. RAW 264.7 cells were incubated with 10 μM seselin or the same volume of DMSO in the presence of 10 ng·mL^{-1} LPS and 10 ng·mL^{-1} IFN-γ, or 20 ng·mL^{-1} IL4, for 6 h, and then stained for STAT1 (G) or p65 (H). The nuclei were stained with DAPI (blue). The line charts represent the mean fluorescence intensity (MFI), which is presented the distance from α to ω in the images in arbitrary units (AU). Scale bar, 10 μm.

2016). This diversity has attracted substantial attention from medicinal chemists for the development of related synthetic agents (Barot *et al.*, 2015). Although many attempts have been made to examine novel structures for biological activities, it is increasingly important to investigate the details of the molecular mechanisms and targets to further strengthen their indication and to avoid unexpected side-effects. Here, we have identified the activity of seselin and further elucidated the underlying mechanisms. Seselin targeted the signalling kinase Jak2 to block the proinflammatory phenotype of macrophages in order to ameliorate inflammatory conditions.

Firstly, we evaluated the *in vivo* anti-inflammatory activity of seselin. Organ dysfunction and assessment of the sequential organ failure has become the new standard for the diagnosis of sepsis, since a new clinical definition was published

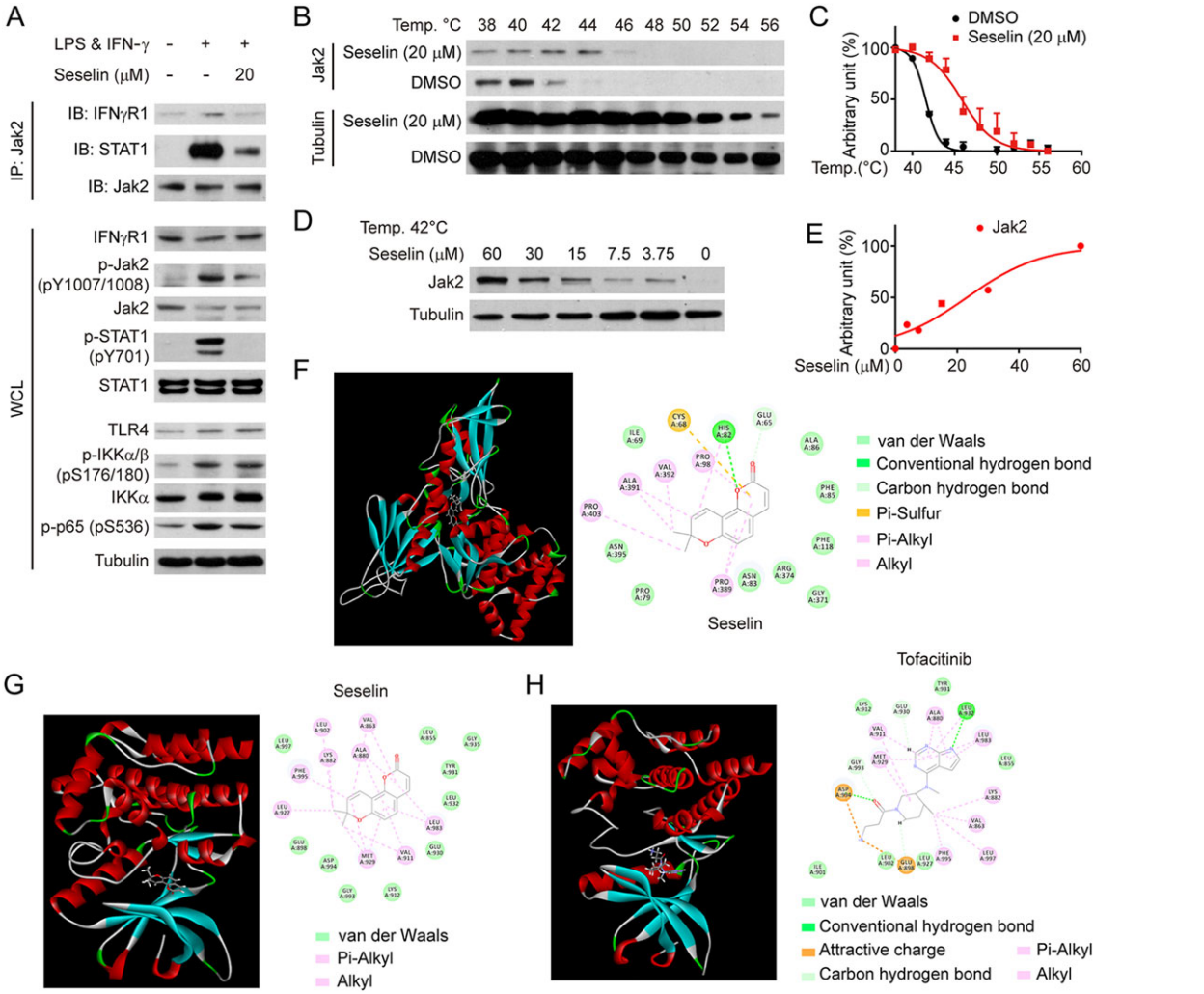

Figure 5

Seselin targeted Jak2 to disrupt the signal transduction. (A) RAW 264.7 cells were incubated with 20 μM seselin in the presence of 10 ng·mL^{-1} LPS and 10 ng·mL^{-1} IFN-γ for 6 h. Interaction between Jak2 and IFNγR or STAT1 was determined by immunoblot after immunoprecipitation with anti-Jak2. Whole cell lysates (WCL) were analysed by Western blot to monitor expression of protein. (B) RAW 264.7 cells were incubated with DMSO or seselin for 2 h. The WCL were assayed with CETSA to analyse the thermal stabilization of Jak2. (C) Data summary of (B) is expressed as scatter plots and the fitting curve of mean ± SEM of five independent experiments. (D) RAW 264.7 cells were incubated with DMSO or various doses of seselin for 2 h. The WCL were analysed by CETSA at 42°C to analyse the thermal stabilization of Jak2. (E) Data summary of (D) was expressed as scatter plots and the fitting curve of mean ± SEM of five independent experiments. (F and G) Molecular docking analysis of seselin and Jak2 at different domains. (H) Molecular docking analysis of tofacitinib and Jak2.

in 2016 (Fujishima, 2016). Lung dysfunction, referred to as acute respiratory distress syndrome or acute lung injury, is frequently associated with sepsis (Fujishima, 2016). For the sepsis patient, it is vital to rebalance the inflammatory response and protect lung tissue. Seselin, in addition to increasing survival of mice with sepsis, also decreased damage to lung tissue and reduced the infiltration of proinflammatory macrophages, which might contribute to better prognosis (Figures 1 and 6). In the lung and alveolar space, inflammation is intimately tied to the functional phenotype of the macrophage. Classically, at least two types of macrophage have been found in lung tissue - alveolar macrophages (AM) and interstitial macrophages. Consistent with earlier reports (Guth *et al.*, 2009; Kopf *et al.*, 2015), our data showed that alveolar macrophages expressed high levels of CD11c, a marker of the proinflammatory macrophages, and formed 90–95% of the cellular content in the steady state (Figure 7A). The most likely reason might be the persistent exposure to airborne pathogens in the air space of the alveoli, where AM was located (Kasahara *et al.*, 2012; Aggarwal *et al.*, 2014). Seselin treatment significantly suppressed the proinflammatory macrophages, both in BALF and in lung tissue. Taking into consideration that seselin only slightly affected the infiltration of neutrophils (Figure 7C and Supporting Information Figure S3B) and the differentiation from monocytes to macrophages (Supporting Information Figure S4A), we believe that the anti-inflammatory activity of seselin was mainly exerted through its regulation of macrophage phenotype.

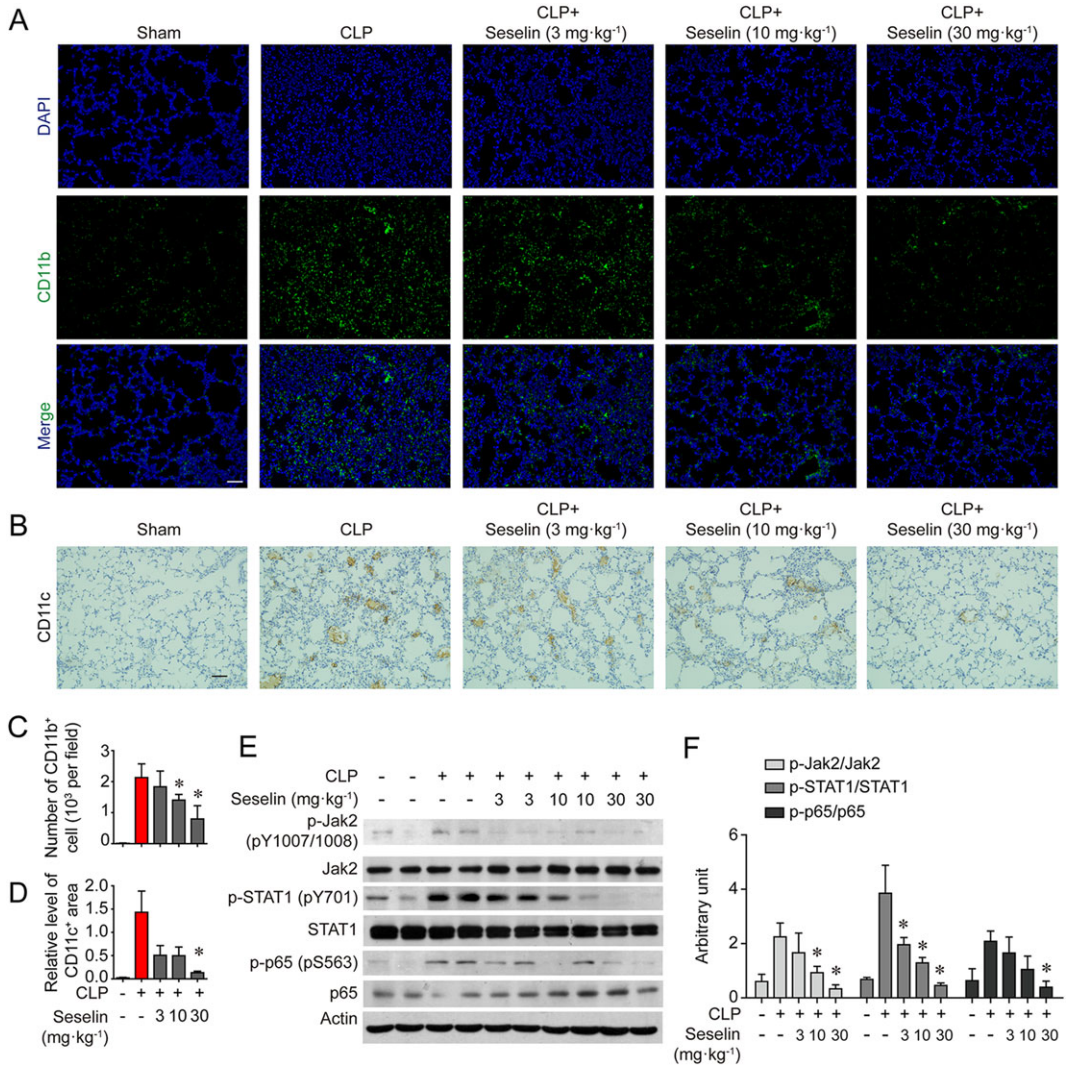

Figure 6

Seselin ameliorated lung injury and decreased JAK2 phosphorylation level in lung tissue during sepsis. (A) Mice were treated as in Figure 1. Four hours after CLP, mice were killed. CD11b expression in lung tissue was detected by immunofluorescence. Scale bar 50 μm. (C) Positive cell numbers of (A) were quantified and is shown as means ± SEM of five fields per mouse in every group. CD11c expression in lung tissue was detected by immunohistochemistry (B) and quantified by ImageJ (D). Scale bar 50 μm. Positive expression was quantified and is shown as means ± SEM of five fields for per mouse in every group. (E) p-Jak2, Jak2, p-STAT1, STAT1, p-p65, p65 and actin expression in lung tissue was detected by Western blot. Actin was a loading control. (F) Data summary of (E) is shown as means ± SEM. n = 10 mice per group. *$P < 0.05$, significantly different from CLP group.

Furthermore, the targeting of macrophage by seselin *in vivo* was further confirmed in our experiments using adoptive transfer of seselin pretreated-BMDMs to macrophage-depleted mice (Figure 8).

Based on the results from the experiments using mice with sepsis, we further comprehensively evaluated the inhibition of seselin in classical activated macrophage in the present study. Thus, seselin decreased both the mRNA and protein levels of proinflammatory factors in concentration and time dependent manner (Figure 2 and Supporting Information Figure S2A). Other functional characteristics of these macrophages, including iNOS expression, phagocytosis and cell surface markers, were also inhibited, further confirming the anti-inflammatory activity of seselin (Figure 3). However, seselin did not affect the cytokine profile of macrophages with anti-inflammatory phenotypes (Supporting Information Figure S2B). This selectivity for the proinflammatory, over the anti-inflammatory phenotype might prevent side-effects *in vivo*, such as secondary infection during the recovery period of sepsis patients.

To confirm the underlying mechanism(s) and the molecular target(s) of seselin, we measured the phosphorylation levels of two transcription factors (STAT1 and p65). Results in Figure 4 suggested seselin exerted a greater inhibition of STAT1, relative to that of p65, as indicated by the relatively slight effect on p-p65. Based on this result, we would propose that seselin mainly modulated the STAT1 signalling pathway rather than that of the NF-κB pathway. We followed up these observations by studying the effect of seselin on upstream interactions between Jak2 and STAT1

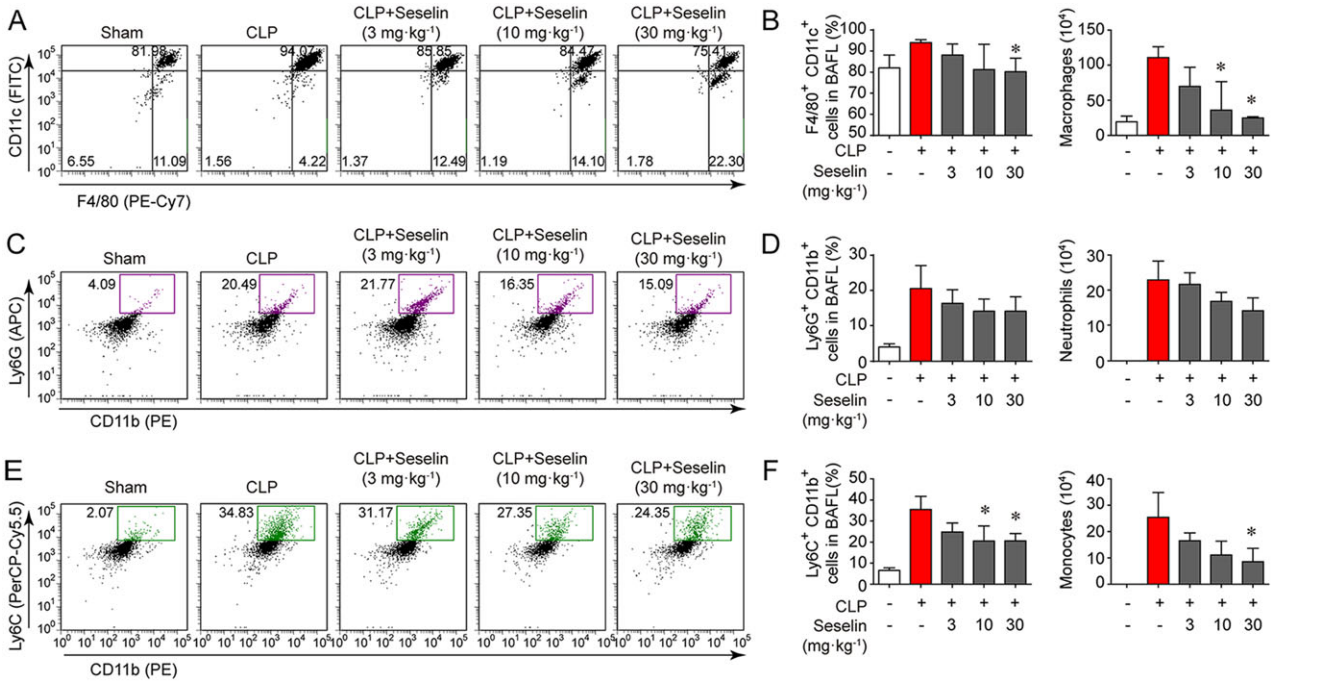

Figure 7

Seselin reduced the immune cell counts in BALF induced by CLP. Mice were treated as in Figure 1. Four hours after the surgery, mice were killed. Cells in BAFL were collected and analysed by flow cytometry. CD45 gated cells were further counted. (A) The percentage of F4/80$^+$CD11c$^+$ macrophages. (B) Data summary of (A) and macrophages counts are shown as means ± SEM. (C) The percentage of CD11b$^+$Ly6G$^+$ neutrophils. (D) Data summary of (C) and neutrophil counts are shown as means ± SEM. (E) The percentage of CD11b$^+$Ly6C$^+$ monocytes. (F) Data summary of (E) and monocyte counts are shown as means ± SEM. n = 10 mice per group. *$P < 0.05$, significantly different from the CLP group.

and the cellular molecular target. Briefly, upon IFN-γ stimulation, Jak2 was recruited and autophosphorylated. The phospho-Jak2 then phosphorylated the oligomerised IFNγR1 at Tyr440 in the cytoplasmic tails, which provide a docking site for the recruitment of STAT1 and to facilitate the subsequent phosphorylation of STAT1 at Tyr701, by phosphorylated JAKs. The p-STAT1 is then translocated to the nucleus to elicit the relevant gene expression (Stark and Darnell, 2012; Villarino *et al.*, 2017). Consistent with its suppression of STAT1, seselin also suppressed the interaction between Jak2 and STAT1 or IFNγR1, as well as p-Jak2, (Figure 5A). CETSA confirmed directly the interaction of seselin with Jak2, as indicated by increased thermal stability of Jak2 in the presence of seselin (Figure 5B–E).

There is growing evidence for the basic and clinical benefits of Jak inhibitors for the understanding of human health and disease. Ruxolitinib was the first Jak inhibitor approved by the US Food and Drug Administration for treatment of myeloproliferative neoplasms that are mainly induced by *JAK2V617F* (Geyer and Mesa, 2014). Recently, tofacitinib was also approved for the treatment of rheumatoid arthritis (O'Shea *et al.*, 2015). And now, these drugs have been tested for a number of malignancies, alopecia areata, ankylosing spondylitis and immunology disorders like psoriasis, lupus and ulcerative colitis, which further exemplified the potential therapeutic value of Jak as a target for drugs. Jak2 inhibitors have been divided into two types based on their mechanisms. Type I JAK inhibitors bind and stabilized the active kinase conformation despite blockade of kinase function, most clinical approved inhibitors belonged to this type (Andraos *et al.*, 2012). Myeloproliferative neoplasm (MPN) cells can acquire an adaptive form of resistance to JAK inhibitors, called "persistence", through reactivation of JAK–STAT signalling *via* heterodimerization and transactivation of Jak2 by JAK1 and TYK2, although the MPN-associated splenomegaly and systemic symptoms were improved (Koppikar *et al.*, 2012). A type II JAK inhibitor was still effective in cells displaying persistence to a type I JAK inhibitor (Andraos *et al.*, 2012; Meyer *et al.*, 2015). In our experiments, unlike type I JAK inhibitors, seselin suppressed the phosphorylation level of Jak2, indicating characteristics of type II JAK inhibitors. However, molecular docking predicted that seselin would have greater affinity for the FERM domain rather than the kinase domain (Figure 5), implying that seselin's anti-inflammatory activity was due to hindrance of the interaction of Jak2 with upstream cytokine receptors. This mode of action differs from that of both type I and type II JAK inhibitors.

However, seselin significantly suppressed expression of IL-1β, IL-6 and TNF-α, usually considered to be regulated by the NF-κB signalling pathway, even though seselin only slightly inhibited p-p65, the crucial component of this pathway (Figures 2 and 4). We suggest this inhibition of cytokines was, in this instance, partly due to inhibition of p-STAT1. It is likely that parallel signalling pathways could influence NF-κB activity as macrophages respond to a wide range of extracellular stimuli. A relationship between STAT1 and NF-κB signalling has long been recognised, as the two

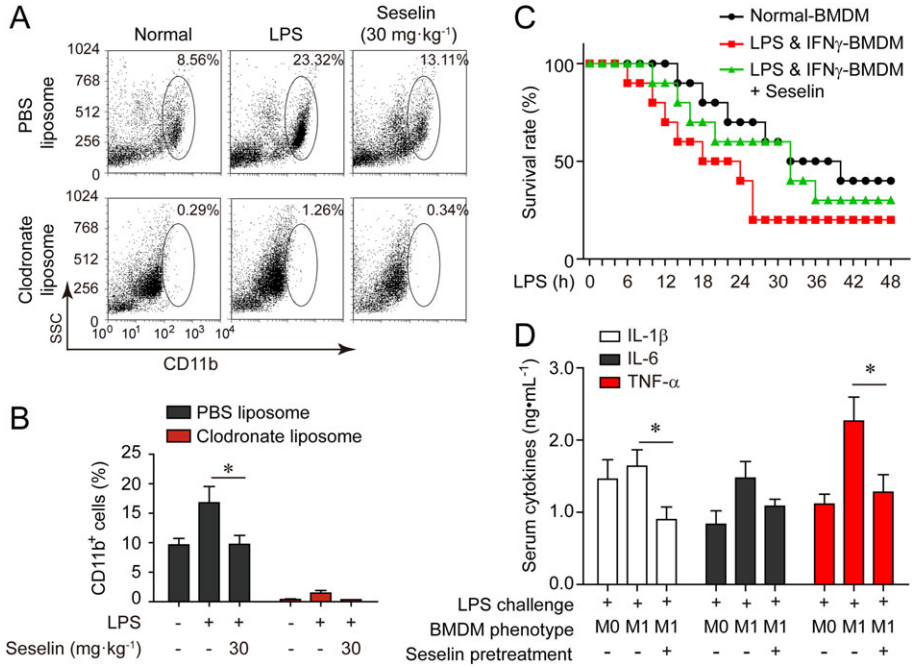

Figure 8

Adoptive transfer of seselin-treated BMDMs ameliorates LPS-induced peritonitis in mice. (A) Clodronate or PBS liposome was injected i.p.. Twenty-four hours later, mice were challenged by LPS (10 mg·kg^{-1}) for 4 h, and the expression of CD11b in peritoneal exudate cells was measured by flow cytometry. (B) Data summary of (A) is shown as means ± SEM. $n = 5$ mice per group. (C) BMDMs were incubated with 20 μM seselin or the same volume of DMSO in the presence of 10 mg·kg^{-1} LPS and 10 mg·kg^{-1} IFN-γ for 6 h. Macrophage depleted mice were treated with Normal-BMDM, LPS and IFN-γ-BMDM or seselin treated LPS and IFN-γ-BMDM (i.v.) and challenged with 10 mg·kg^{-1} LPS (i.p.). Survival was measured . (D) Mice were treated as (C). Four hours later, serum cytokines were measured by ELISA. $n = 10$ mice per group. *$P < 0.05$, significantly different as indicated.

pathways can promote or prime each other (Yarilina *et al.*, 2008; Ivashkiv and Donlin, 2014). Although we cannot exclude the possibility of additional targets of seselin, the malfunction of the Jak2-STAT1 pathway following disruption of Jak2 activity would explain the major effects on macrophage phenotype.

Because of the effects of phenotype plasticity and complexity on homeostasis and diseases involving macrophages, targeting macrophages and interfering with their functional properties has become a promising therapeutic option for the treatment of inflammatory diseases. Here, we have shown the anti-inflammatory activity of seselin in macrophages. Our results suggest that seselin might bind to the FERM domain of Jak2 to disrupt its interaction with upstream IFNγR, thus suppressing STAT1 activity and the proinflammatory phenotype of macrophages. Our data has identified a promising therapeutic agent for inflammatory diseases, effective *via* modulated Jak2 activity. Our data has also widened the application of Jak2 inhibitors, although there is still much more work needed to confirm the details of the binding of the compound with Jak2 and the related molecular events.

Acknowledgements

This work was supported by National Natural Science Foundation of China (nos. 81673487, 81473221, 81330079, 81872916, 21472091, 81670553 and 81722047) and Natural Science Foundation of Jiangsu Province (BK20161399).

Author contributions

The study conception, design and manuscript writing were performed by X.W., L.F. and Q.X. The acquisition, analysis and/or interpretation of data were carried out by L.F., Y.S., P.S., L.X., X.W., X.W., Y.S., Y.S., and L.K. The final approval and overall responsibility for the published work were carried out by X.W. and Q.X.

Conflict of interest

The authors declare no conflicts of interest.

Declaration of transparency and scientific rigour

This Declaration acknowledges that this paper adheres to the principles for transparent reporting and scientific rigour of preclinical research recommended by funding agencies, publishers and other organisations engaged with supporting research.

References

Aggarwal NR, King LS, D'Alessio FR (2014). Diverse macrophage populations mediate acute lung inflammation and resolution. Am J Physiol Lung Cell Mol Physiol 306: L709–L725.

Aldo PB, Craveiro V, Guller S, Mor G (2013). Effect of culture conditions on the phenotype of THP-1 monocyte cell line. American journal of reproductive immunology (New York, NY: 1989) 70: 80–86.

Alexander SPH, Fabbro D, Kelly E, Marrion NV, Peters JA, Faccenda E *et al*. (2017a). The Concise Guide to PHARMACOLOGY 2017/18: Enzymes. Br J Pharmacol 174 (Suppl. 1): S272–S359.

Alexander SPH, Kelly E, Marrion NV, Peters JA, Faccenda E, Harding SD *et al*. (2017b). The Concise Guide to PHARMACOLOGY 2017/18: Other proteins. Br J Pharmacol 174 (Suppl. 1): S1–S16.

Alexander SPH, Fabbro D, Kelly E, Marrion NV, Peters JA, Faccenda E *et al*. (2017c). The Concise Guide to PHARMACOLOGY 2017/18: Catalytic receptors. Br J Pharmacol 174: S225–S271.

Alvarez-Errico D, Vento-Tormo R, Sieweke M, Ballestar E (2015). Epigenetic control of myeloid cell differentiation, identity and function. Nat Rev Immunol 15: 7–17.

Anand P, Singh B, Singh N (2012). A review on coumarins as acetylcholinesterase inhibitors for Alzheimer's disease. Bioorg Med Chem 20: 1175–1180.

Andraos R, Qian Z, Bonenfant D, Rubert J, Vangrevelinghe E, Scheufler C *et al*. (2012). Modulation of activation-loop phosphorylation by JAK inhibitors is binding mode dependent. Cancer Discov 2: 512–523.

Barot KP, Jain SV, Kremer L, Singh S, Ghate MD (2015). Recent advances and therapeutic journey of coumarins: current status and perspectives. Med Chem Res 24: 2771–2798.

Benoit M, Desnues B, Mege JL (2008). Macrophage polarization in bacterial infections. J Immunol 181: 3733–3739.

Bozza FA, Salluh JI, Japiassu AM, Soares M, Assis EF, Gomes RN *et al*. (2007). Cytokine profiles as markers of disease severity in sepsis: a multiplex analysis. Crit Care 11: R49.

Buras J, Holzmann B, Sitkovsky M (2005). Animal models of sepsis: setting the stage. Nat Rev Drug Discov 4: 854–865.

Cardenas-Ortega NC, Perez-Gonzalez C, Zavala-Sanchez MA, Hernandez-Ramirez AB, Perez-Gutierrez S (2007). Antifungal activity of seselin in protecting stored maize from Aspergillus flavus. Asian J Plant Sci 6 (4): 712–714.

Cervantes F, Vannucchi AM, Kiladjian JJ, Al-Ali HK, Sirulnik A, Stalbovskaya V *et al*. (2013). Three-year efficacy, safety, and survival findings from COMFORT-II, a phase 3 study comparing ruxolitinib with best available therapy for myelofibrosis. Blood 122: 4047–4053.

Curtis MJ, Alexander S, Cirino G, Docherty JR, George CH, Giembycz MA *et al*. (2018). Experimental design and analysis and their reporting II: updated and simplified guidance for authors and peer reviewers. Brit J Pharmacol 175: 987–993.

Feng L, Song P, Zhou H, Li A, Ma Y, Zhang X *et al*. (2014). Pentamethoxyflavanone regulates macrophage polarization and ameliorates sepsis in mice. Biochem Pharmacol 89: 109–118.

Fleischmann R, Kremer J, Cush J, Schulze-Koops H, Connell CA, Bradley JD *et al*. (2012). Placebo-controlled trial of tofacitinib monotherapy in rheumatoid arthritis. N Engl J Med 367: 495–507.

Fujishima S (2016). Organ dysfunction as a new standard for defining sepsis. Inflamm Regen 36: 24.

Garcia-Argaez AN, Apan TOR, Delgado HP, Velázquez G, Martínez-Vázquez M (2000). Anti-inflammatory activity of coumarins from Decatropis bicolor on TPA ear mice model. Planta Med 66: 279–281.

Geyer HL, Mesa RA (2014). Therapy for myeloproliferative neoplasms: when, which agent, and how? Blood 124: 3529–3537.

Glass CK, Natoli G (2016). Molecular control of activation and priming in macrophages. Nat Immunol 17: 26–33.

Gomez-Outes A, Suarez-Gea ML, Calvo-Rojas G, Lecumberri R, Rocha E, Pozo-Hernandez C *et al*. (2012). Discovery of anticoagulant drugs: a historical perspective. Curr Drug Discov Technol 9: 83–104.

Goren R, Tomer E (1971). Effects of seselin and coumarin on growth, indoleacetic acid oxidase, and peroxidase, with special reference to cucumber (Cucumis sativa L.) radicles. Plant Physiol 47: 312–316.

Grover J, Jachak SM (2015). Coumarins as privileged scaffold for anti-inflammatory drug development. RSC Adv 5: 38892–38905.

Guth AM, Janssen WJ, Bosio CM, Crouch EC, Henson PM, Dow SW (2009). Lung environment determines unique phenotype of alveolar macrophages. Am J Physiol Lung Cell Mol Physiol 296: L936–L946.

Harding SD, Sharman JL, Faccenda E, Southan C, Pawson AJ, Ireland S *et al*. (2018). The IUPHAR/BPS guide to pharmacology in 2018: updates and expansion to encompass the new guide to immunopharmacology. Nucl Acids Res 46: D1091–D1106.

Hernanz R, Martinez-Revelles S, Palacios R, Martin A, Cachofeiro V, Aguado A *et al*. (2015). Toll-like receptor 4 contributes to vascular remodelling and endothelial dysfunction in angiotensin II-induced hypertension. Br J Pharmacol 172: 3159–3176.

Ivashkiv LB, Donlin LT (2014). Regulation of type I interferon responses. Nat Rev Immunol 14: 36–49.

Jafari R, Almqvist H, Axelsson H, Ignatushchenko M, Lundback T, Nordlund P *et al*. (2014). The cellular thermal shift assay for evaluating drug target interactions in cells. Nat Protoc 9: 2100–2122.

Jha AK, Huang SC, Sergushichev A, Lampropoulou V, Ivanova Y, Loginicheva E *et al*. (2015). Network integration of parallel metabolic and transcriptional data reveals metabolic modules that regulate macrophage polarization. Immunity 42: 419–430.

Kasahara K, Matsumura Y, Ui K, Kasahara K, Komatsu Y, Mikasa K *et al*. (2012). Intranasal priming of newborn mice with microbial extracts increases opsonic factors and mature CD11c+ cells in the airway. Am J Physiol Lung Cell Mol Physiol 303: L834–L843.

Kilkenny C, Browne W, Cuthill IC, Emerson M, Altman DG (2010). Animal research: reporting *in vivo* experiments: the ARRIVE guidelines. Br J Pharmacol 160: 1577–1579.

Kopf M, Schneider C, Nobs SP (2015). The development and function of lung-resident macrophages and dendritic cells. Nat Immunol 16: 36–44.

Koppikar P, Bhagwat N, Kilpivaara O, Manshouri T, Adli M, Hricik T *et al*. (2012). Heterodimeric JAK-STAT activation as a mechanism of persistence to JAK2 inhibitor therapy. Nature 489: 155–159.

Kostova I, Bhatia S, Grigorov P, Balkansky S, Parmar VS, Prasad AK *et al*. (2011). Coumarins as antioxidants. Curr Med Chem 18: 3929–3951.

Kotas ME, Medzhitov R (2015). Homeostasis, inflammation, and disease susceptibility. Cell 160: 816–827.

Lawrence T, Natoli G (2011). Transcriptional regulation of macrophage polarization: enabling diversity with identity. Nat Rev Immunol 11: 750–761.

Lima V, Silva CB, Mafezoli J, Bezerra MM, Moraes MO, Mourão GS *et al*. (2006). Antinociceptive activity of the pyranocoumarin seselin in mice. Fitoterapia 77: 574–578.

Martin GS, Mannino DM, Eaton S, Moss M (2003). The epidemiology of sepsis in the United States from 1979 through 2000. N Engl J Med 348: 1546–1554.

Matsunaga N, Tsuchimori N, Matsumoto T, Ii M (2011). TAK-242 (resatorvid), a small-molecule inhibitor of Toll-like receptor (TLR) 4 signaling, binds selectively to TLR4 and interferes with interactions between TLR4 and its adaptor molecules. Mol Pharmacol 79: 34–41.

McGrath JC, Lilley E (2015). Implementing guidelines on reporting research using animals (ARRIVE etc.): new requirements for publication in BJP. Br J Pharmacol 172: 3189–3193.

Melliou E, Magiatis P, Mitaku S, Skaltsounis AL, Chinou E, Chinou I (2005). Natural and synthetic 2,2-dimethylpyranocoumarins with antibacterial activity. J Nat Prod 68: 78–82.

Meyer SC, Keller MD, Chiu S, Koppikar P, Guryanova OA, Rapaport F *et al*. (2015). CHZ868, a Type II JAK2 inhibitor, reverses type I JAK inhibitor persistence and demonstrates efficacy in myeloproliferative neoplasms. Cancer Cell 28: 15–28.

Meylan E, Tschopp J, Karin M (2006). Intracellular pattern recognition receptors in the host response. Nature 442: 39–44.

O'Shea JJ, Schwartz DM, Villarino AV, Gadina M, McInnes IB, Laurence A (2015). The JAK-STAT pathway: impact on human disease and therapeutic intervention. Annu Rev Med 66: 311–328.

Piccolo V, Curina A, Genua M, Ghisletti S, Simonatto M, Sabo A *et al*. (2017). Opposing macrophage polarization programs show extensive epigenomic and transcriptional cross-talk. Nat Immunol 18: 530–540.

Rittirsch D, Hoesel LM, Ward PA (2007). The disconnect between animal models of sepsis and human sepsis. J Leukoc Biol 81: 137–143.

Rittirsch D, Huber-Lang MS, Flierl MA, Ward PA (2008). Immunodesign of experimental sepsis by cecal ligation and puncture. Nat Protoc 4: 31.

Riveiro ME, De Kimpe N, Moglioni A, Vazquez R, Monczor F, Shayo C *et al*. (2010). Coumarins: old compounds with novel promising therapeutic perspectives. Curr Med Chem 17: 1325–1338.

Rodgaard-Hansen S, Rafique A, Christensen PA, Maniecki MB, Sandahl TD, Nexo E *et al*. (2014). A soluble form of the macrophage-related mannose receptor (MR/CD206) is present in human serum and elevated in critical illness. Clin Chem Lab Med 52: 453–461.

Schwende H, Fitzke E, Ambs P, Dieter P (1996). Differences in the state of differentiation of THP-1 cells induced by phorbol ester and 1,25-dihydroxyvitamin D3. J Leukoc Biol 59: 555–561.

Sica A, Mantovani A (2012). Macrophage plasticity and polarization: *in vivo* veritas. J Clin Invest 122: 787–795.

Siriwardhana A, Wijesundara S, Karunaratne V (2015). A review of studies on bioactive compounds isolated from Sri Lankan flora. J Natl Sci Found 43: 11.

Spellberg B, Edwards JE (2002). The pathophysiology and treatment of *Candida* sepsis. Curr Infect Dis Rep 4: 387–399.

Stark GR, Darnell JE Jr (2012). The JAK-STAT pathway at twenty. Immunity 36: 503–514.

Stearns-Kurosawa DJ, Osuchowski MF, Valentine C, Kurosawa S, Remick DG (2011). The pathogenesis of sepsis. Annu Rev Pathol 6: 19–48.

Vera B, Rodriguez AD, La Clair JJ (2011). Aplysqualenol A binds to the light chain of dynein type 1 (DYNLL1). Angew Chem Int Ed Engl 50: 8134–8138.

Villarino AV, Kanno Y, O'Shea JJ (2017). Mechanisms and consequences of Jak-STAT signaling in the immune system. Nat Immunol 18: 374–384.

Xu G, Feng L, Song P, Xu F, Li A, Wang Y*et al*. (2016). Isomeranzin suppresses inflammation by inhibiting M1 macrophage polarization through the NF-κB and ERK pathway. Int Immunopharmacol 38: 175–185.

Yarilina A, Park-Min KH, Antoniv T, Hu X, Ivashkiv LB (2008). TNF activates an IRF1-dependent autocrine loop leading to sustained expression of chemokines and STAT1-dependent type I interferon-response genes. Nat Immunol 9: 378–387.

Yu YR, O'Koren EG, Hotten DF, Kan MJ, Kopin D, Nelson ER *et al*. (2016). A protocol for the comprehensive flow cytometric analysis of immune cells in normal and inflamed murine non-lymphoid tissues. PloS one 11: e0150606.

Supporting Information

Additional supporting information may be found online in the Supporting Information section at the end of the article.

https://doi.org/10.1111/bph.14521

Figure S1 Effect of seselin on cell viability and proliferation. BMDM were incubated with various dose of compounds or the same volume of DMSO in the absence (A) or presence of 10 ng·ml-1 LPS and 10 ng·ml-1 IFN-γ (B) or 20 ng·ml-1 IL-4 (C) for 24 h. Cell viability was detected by MTT assay. Data were expressed as a histogram of mean ± SEM of five independent experiments. (D) Raw 264.7 cells were incubated as (B and C) after staining CFSE. Cell proliferation was detected by Flow cytometry.

Figure S2 Effect of seselin on macrophage phenotype. (A) BMDMs were treated with 20 μM compounds or the same volume of DMSO in the presence of 10 ng·ml-1 LPS and 10 ng·ml-1 IFN-γ (the proinflammatory phenotype) for 6 h. The mRNA levels of *Il-12*, *Ccl3*, *Ccl7*, *Cxcl9* and *Cxcl1* were determined by quantitative PCR. $^{*}P < 0.05$ *vs*. LPS & IFN-γ treated group. (B) BMDMs were treated with 20 μM compounds or the same volume of DMSO in the presence of 20 ng·ml-1 IL-4 (the anti-inflammatory phenotype) for 6 h. The mRNA levels of *Arg1*, *Fizz1*, *Ym1*, *Ccl17*, *Ccl22* and *Cd163* were determined by quantitative PCR. Data were expressed as a histogram of mean ± SEM of five independent experiments.

Figure S3 Seselin reduced the immune cell counts in lung tissue. Mice were treated as in Figure 1.4 hours after the surgery, mice were sacrificed. Cells in lung tissue were collected and analyzed by Flow cytometry. CD45+ gated cells were

further detected. (A) The percentage of F4/80+CD11c+ macrophages. Data summary expressed as a histogram of mean ± SEM. (B) The percentage of Ly6G+ neutrophils. Data summary was expressed as a histogram of mean ± SEM. (C) The percentage of CD11b+Ly6C+ monocytes. Data summary was expressed as a histogram of mean ± SEM. n = 10 mice per group. *$P < 0.05$ *vs*. CLP group.

Figure S4 Effect of seselin on the differentiation of THP-1 monocytes and the following activation. THP-1 was stimulated with 500 nM PMA for 24 hours in the presence of various dose of seselin. (A) CD14 expression was detected by flow cytometry. (B) Data summary of (A) was expressed as a histogram of mean ± SEM. *$P < 0.05$ *vs*. PMA treated group. (C) THP-1 was stimulated with 500 nM PMA for 3 hours followed by activation with 100 ng·ml-1 LPS and 100 ng·ml-1 IFN-γ in the presence of various dose of seselin for 6 hours. The mRNA levels of *IL-6* and *TNF-α* were determined by quantitative PCR. *$P < 0.05$ *vs*. LPS and IFN-γ treated group.